

*Faculty of Engineering*  
*Faculty of Engineering - Papers*

---

*University of Wollongong*

*Year 2002*

---

Analysis of Critical Hydraulic Gradient  
for Particle Movement in Filtration

B. Indraratna\*      S. Radampola†

\*University of Wollongong, [indra@uow.edu.au](mailto:indra@uow.edu.au)

†University of Wollongong

This article was originally published as: Indraratna, B & Radampola, S, Analysis of Critical Hydraulic Gradient for Particle Movement in Filtration, Journal of Geotechnical and Geoenvironmental Engineering, 2002, 128(4), 347-350. Copyright American Society of Civil Engineers. Original journal available <[a href="http://scitation.aip.org/gto"](http://scitation.aip.org/gto)>here</a>.

This paper is posted at Research Online.

<http://ro.uow.edu.au/engpapers/178>

# Analysis of Critical Hydraulic Gradient for Particle Movement in Filtration

Buddhima Indraratna, M.ASCE,<sup>1</sup> and Sujeewa Radampola<sup>2</sup>

**Abstract:** The objective of this paper is to propose an explicit solution for the critical hydraulic gradient required to move a base particle within a pore channel. The particle is assumed to displace when the applied hydrodynamic forces exceed this critical hydraulic gradient. The current analysis is an extension of a previous study (Indraratna and Vafai 1997), where the limit equilibrium analysis was modified to include the effect of drag in the hydrodynamic force component. The theoretical model was examined in the laboratory using fine gravel filters and a cohesionless base soil consisting of very fine river sand.

**DOI:** 10.1061/(ASCE)1090-0241(2002)128:4(347)

**CE Database keywords:** Filters; Filtration; Dams, embarkment; Erosion; Hydraulic Gradients; Seepage; Porous media.

## Introduction

An assemblage of unconnected fluid conduits, model the pore system geometry resulting from granular packing of discrete particles. As shown in Fig. 1, these conduits are parallel to the flow direction, and the minimum pore diameter ( $d_0$ ) is determined by the following expression (Kovacs 1981):

$$d_0 = 2.67 \frac{n}{1-n} \frac{D_h}{\alpha} \quad (1a)$$

where  $\alpha$  = shape coefficient;  $n$  = porosity; and

$$D_h = \frac{1}{\sum \frac{\Delta S_i}{D_i}} \quad (1b)$$

In the previous equation,  $D_i$  = average diameter in the  $i$ th interval of the particle size distribution curve of the sample considered and  $\Delta S_i$  = weight of grains in the  $i$ th interval divided by the total weight of the sample (Fig. 2).

Using Poiseuille's equation, the flow ( $Q_0$ ) through one pore channel in the model is given by

$$Q_0 = \pi \left( \frac{\gamma_w}{\mu_w} \right) \left( \frac{d_0^4}{128} \right) i \quad (2)$$

where  $i$  = hydraulic gradient and  $\mu_w$  and  $\gamma_w$  are the viscosity and the unit weight of water, respectively.

<sup>1</sup>Professor, Division of Civil Engineering, Univ. of Wollongong, NSW 2522, Australia. E-mail: b.indraratna@uow.edu.au or indra@uow.edu.au

<sup>2</sup>Research Fellow, Division of Civil Engineering, Univ. of Wollongong, NSW 2522, Australia.

Note. Discussion open until September 1, 2002. Separate discussions must be submitted for individual papers. To extend the closing date by one month, a written request must be filed with the ASCE Managing Editor. The manuscript for this technical note was submitted for review and possible publication on November 7, 2000; approved on August 18, 2001. This technical note is part of the *Journal of Geotechnical and Geoenvironmental Engineering*, Vol. 128, No. 4, April 1, 2002. ©ASCE, ISSN 1090-0241/2002/4-347-350/\$8.00+\$0.50 per page.

The number of pores in the model ( $N$ ) crossing the unit area of the sample is given by

$$N = \frac{4n}{\pi d_0^2} \quad (3)$$

Thus, the virtual discharge velocity ( $v$ ) of the sample becomes

$$v = Q_0 N = n \left( \frac{\gamma_w}{\mu_w} \right) \left( \frac{d_0^2}{32} \right) i \quad (4)$$

Comparing the above equation with Darcy's law,  $v = ki$ , the hydraulic conductivity ( $k$ ) is given by

$$k = n \left( \frac{\gamma_w}{\mu_w} \right) \left( \frac{d_0^2}{32} \right) \quad (5)$$

Pressure and viscous (drag) forces due to flow act on a stationary particle immersed in flowing water. Other than these, the gravity and uplift forces as well as the frictional resistance also act on the particle [Fig. 3(a)]. Once the applied forces on the particle reach a critical value exceeding the resisting forces, along any given

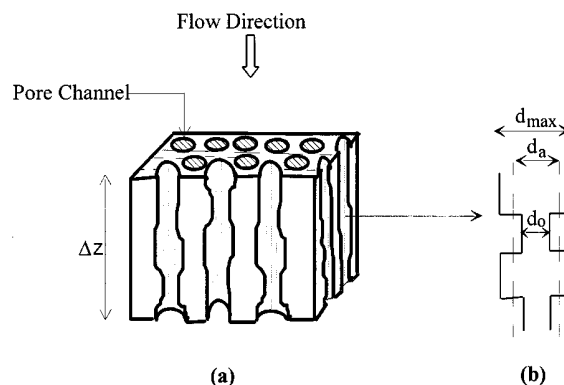


**Fig. 1.** Illustration of (a) pore channels within typical filter element; (b) section of pore channel defining the minimum equivalent pore diameter,  $d_0$  (Indraratna and Fafai 1997)

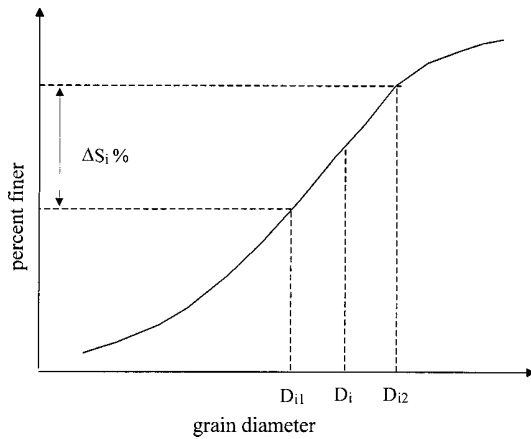


**Fig. 2.** Calculation of effective diameter from particle size distribution curve

direction, the particle is assumed to move. The movement of a particle (maximum dimension less than the pore diameter,  $d_0$ ) can be described according to three possibilities:

1. The particle will either propagate through a certain distance and then become stationary again, or
2. It will be completely washed out from the system, or
3. It will stop when it reaches a smaller pore or a pore comparable to its size.

The above situations will be elaborated in the following section.

### Force Balancing of a Particle

The pore system is modeled as an assemblage of fluid conduits with a minimum pore diameter ( $d_0$ ) given by Eq. (1a). The size of the base particle that can pass through a pore channel is governed by the smallest of the constriction  $d_0$  within the pore channel geometry. Indraratna and Vafai (1997) have adopted a model

representing the voids in a filter as parallel channels of constriction (Fig. 1), which is also followed here. The use of pore constriction,  $d_0$  was shown by Kovacs (1981), as an appropriate characterization of the effective pore sizes of a natural soil to study the retention of fine grains in granular soil pores. Thus, the minimum pore diameter  $d_0$  (constriction) is adopted in this paper, as it is assumed to be the most influencing factor, which governs the size of erodible base particle.

Transient phenomena such as consolidation, swelling or shrinkage of soil matrix will not be considered within the scope of this analysis. Fluid flow is assumed to be incompressible, and the pore system is assumed to be saturated. The inertial forces are neglected.

Consider a pore element of diameter ( $d_0$ ) centered on a streamline representing its bearing at an angle  $\alpha$  to the horizontal axis (Fig. 3). It contains a base particle of diameter ( $d$ ) in contact with the pore channel wall. Steady state flow through the pore element is assumed.

### Case 1: $d < d_0$ (Fig. 3)

Limit equilibrium in the direction of flow results in the following equation:

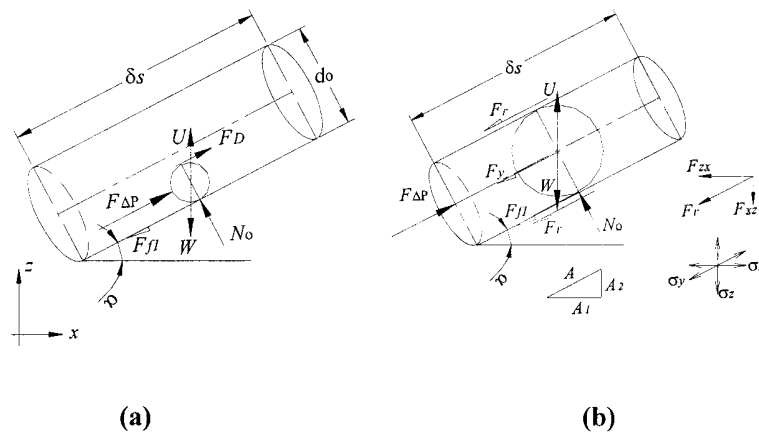
$$F_{\Delta P} + F_D - (W - U) \sin \alpha - F_{f1} = 0 \quad (6)$$

$F_D$  denotes the drag force of particle,  $F_{f1}$  is the shear (frictional) force at the interface of the particle and the pore wall,  $W$  is the weight of the particle and  $U$  is the uplift force.  $F_{\Delta P}$  denotes the net hydrostatic force acting on the projected surface area of the particle.

Hydrostatic force ( $F_{\Delta P}$ ) can be calculated considering Darcy's law, from which the following equation can be derived after mathematical simplification:

$$F_{\Delta P} = i \gamma_w (\delta s) \left( \frac{\pi d^2}{4} \right) \quad (7)$$

where  $\delta s$  = length of pore channel.



**Note:**

$$F_{f1} = (W - U) \cos \alpha \tan \phi'$$

$$F_y = 0.5 \pi d^2 K (\gamma_s h_s - \gamma_w h_w) \tan \phi'$$

$$F_r = \sqrt{F_{xz}^2 + F_{zx}^2} \text{ where}$$

$$F_{zx} = 0.5 \pi d^2 K (\gamma_s h_s - \gamma_w h_w) \sin \alpha \tan \phi'$$

$$F_{xz} = 0.5 \pi d^2 (\gamma_s h_s - \gamma_w h_w) \cos \alpha \tan \phi'$$

**Fig. 3.** Diagram indicating the forces acting on a particle: (a) Case 1: when particle diameter < pore diameter; (b) case 2: when particle diameter = pore diameter

Drag force ( $F_D$ ) is calculated from the Stokes law. If the particle is assumed to achieve terminal velocity and follow laminar flow for Reynolds number less than 0.5, the magnitude of  $F_D$  can be estimated from the following expression:

$$F_D = 3\pi\mu_w d \left(\frac{k}{n}\right) i \quad (8)$$

Frictional force ( $F_{f1}$ ) is calculated as a function of the normal force ( $N_0$ ), acting at the particle-pore wall interface.

Substituting the relevant values for the uplift force ( $U$ ) and weight ( $W$ ) of the particle, an algebraic expression for  $F_{f1}$  is obtained by

$$F_{f1} = \frac{\pi d^3}{6} (\gamma_s - \gamma_w) \cos \alpha (f), \quad (9)$$

where  $f$  = coefficient of friction of the base material =  $\tan \phi$ . The parameter  $\phi$  is the angle of repose of the base material and the term  $(\gamma_s - \gamma_w)$  represents the submerged unit weight ( $\gamma'$ ).

Substituting Eqs. (5) and (7)–(9) in Eq. (6), the value of the hydraulic gradient ( $i$ ) is obtained from

$$i = \frac{2}{3\gamma_w} \frac{d^2}{(\delta_s \cdot d + 0.375 \cdot d_0^2)} (\gamma') [\cos \alpha (f) + \sin \alpha] \quad (10)$$

At the limit when  $\delta_s \rightarrow d$ , the critical hydraulic gradient ( $i_{cr}$ ) is given by

$$i_{cr} = \frac{2}{3\gamma_w} \frac{d^2}{(d^2 + 0.375 \cdot d_0^2)} (\gamma') [\cos \alpha (f) + \sin \alpha] \quad (11)$$

### Case 2: “Plugged” Particle [Fig. 3(b)]

Case 1 was concerned with particles smaller than the pore channel, i.e.,  $d < d_0$ . A special case of this analysis is when the particle becomes fully “plugged” in the pore channel ( $d = d_0$ ). In this situation, the contact frictional forces between the particle surface and the pore wall ( $F_r$  and  $F_y$ ) need to be considered, apart from the force ( $F_{f1}$ ). As previously analyzed by Indraratana and Vafai (1997), in this case, the flow cannot go past the particle, hence, no drag force is accounted for. Therefore the critical hydraulic gradient for a “plugged” base particle for all  $\delta_s > d$  is given by

$$i_{cr} = \frac{2}{\delta_s \gamma_w} (\gamma_s h_s - \gamma_w h_w) \tan \phi' [K + \sqrt{\cos^2 \alpha + K^2 \sin^2 \alpha}] + \frac{2}{3} \frac{d}{(\delta_s \gamma_w)} (\gamma') [\cos \alpha \tan \phi' + \sin \alpha] \quad (12)$$

where  $h_s$  = overburden depth;  $h_w$  = hydraulic head; and  $K = \tan^2(\pi/4 - \phi'/2)$ , where  $0 < K < \tan^2(\pi/4 - \phi'/2)$  and  $\phi'$  = effective friction angle of soil corresponding to Mohr-Coulomb state of stress. Here the effective friction angle is interpreted as the drained friction angle of the media since both base soil and filter materials are assumed to be cohesionless.

In Eq. (12), the value of  $i_{cr}$  is clearly much larger, because of the need to overcome the frictional resistance generated as a function of  $K$ . The value of  $K$  cannot exceed the theoretical maximum governed by the Rankine State. For the condition of “friction free” motion ( $K = 0$  or  $d < d_0$ ), for  $\delta_s > d$ , Eq. (12) simplifies to

$$i_{cr} = \frac{2}{3} \frac{d}{(\delta_s \gamma_w)} (\gamma') [\cos \alpha \tan \phi' + \sin \alpha] \quad (13)$$

The upper bound of  $i_{cr}$  in Eq. (13) occurs at the limit when  $\delta_s = d$  which simply gives the minimum friction originating from

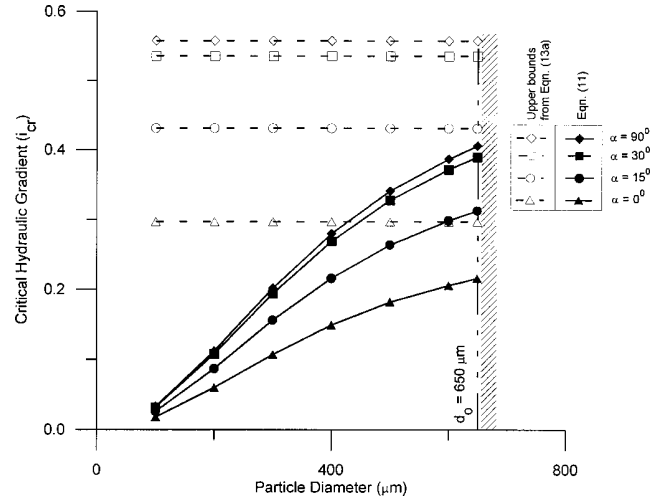


Fig. 4. No erosion boundaries based on critical hydraulic gradients for  $d < d_0$ , for a constant  $d_0$  value of ( $650 \mu\text{m}$ )

the weight and uplift of the base particle ( $F_{f1}$ ). In this situation, the surface friction is the key parameter rather than the effective internal angle of friction. In view of this, it is assumed that the friction factor  $f$  represents a value close to the angle of repose. Thus,  $\tan \phi'$  in Eq. (13) is replaced with the coefficient of friction ( $f$ )

$$i_{cr} = \frac{2}{3} \frac{(\gamma')}{(\gamma_w)} [\cos \alpha (f) + \sin \alpha] \quad (13a)$$

For an assumed angle of repose ( $\phi$ ) of  $28^\circ$ , and submerged unit weight ( $\gamma'$ ) of  $8.2 \text{ kN/m}^3$ , these theoretical upper bounds are plotted in Fig. 4 for  $\alpha$  varying from  $0$  to  $90^\circ$  (horizontal lines with open symbols). Fig. 4 also shows the variation of  $i_{cr}$  with the particle diameter based on Eq. (11) for an equivalent pore diameter of  $650 \mu\text{m}$ . The difference between Eqs. (11) and (13a) represents the effect of the drag force included in the former.

In developing Eq. (11) to determine  $i_{cr}$ , the force balancing is carried out for the condition when filter thickness reaches the particle diameter, i.e., between the two faces of the particle normal to flow. In reality, for a filter to fail, the base particles should reach the downstream boundary of the filter. Therefore, in predicting the actual behavior of a filter, if  $d_0$  is constant throughout filter thickness, then Eq. (11) becomes

$$(i_{cr})_{\text{filter}} = \frac{2}{3\gamma_w} \frac{d \cdot \delta_s}{(d^2 + 0.375 \cdot d_0^2)} (\gamma') [\cos \alpha (f) + \sin \alpha] \quad (14)$$

### Experimental Verification

To compare the model predictions with an actual base soil-filter system, a series of laboratory tests were carried out. A cylindrical filtration apparatus (diameter:  $15.5 \text{ cm}$ ; height:  $24.5 \text{ cm}$ ) with an inlet pressure gauge ( $0$ – $250 \text{ kPa}$ ) was used. The base material consisted of a uniform fine sand ( $C_u = 1.2$ ) in the particle size range of  $212$ – $300 \mu\text{m}$ . The properties of five different uniform filters are given in Table 1. The average thickness of the filter was kept at  $6 \text{ cm}$ , consisting of fine river gravel, compacted in two,  $3 \text{ cm}$  thick layers under a surcharge load of  $9 \text{ kg}$ , and vibrated to achieve the required porosity. The filter depth was chosen as  $6$

**Table 1.** Properties of Uniform Filters Tested

Filter no.	Uniformity coefficient ( $C_u$ )	Grain size (mm)	Porosity ( $n$ ) (%)	Computed pore diameter ( $d_0$ ) ( $\mu\text{m}$ )
1	1.20	2.36–3.35	26.6	456.11
2	1.20	2.36–3.35	29.8	581.28
3	1.45	2.36–4.75	30.0	650.15
4	1.10	3.35–4.00	35.0	876.77
5	1.10	3.35–4.00	39.1	1046.77

cm, to ensure stability under increased hydraulic pressure. Also, a sufficient length was required to calculate the average porosity of the filter medium.

In order to determine the critical hydraulic gradient, the hydraulic pressure was applied to the top of the filtration chamber by increasing the inlet water pressure by small increments of 5–10 kPa. For a typical test subjected to 10 kPa pressure increments, the resulting hydraulic gradients are shown in Fig. 5. At each applied hydraulic gradient, the corresponding flow rate was measured continuously, and the effluent turbidity was monitored using a turbidity meter. Initially, for a very small period of time, a high effluent turbidity was observed, as rapid wash-out of some base soil occurred, prior to the formation of a self-filtering layer at the base soil-filter interface. The formation of a stable interface was evident from decreasing levels of turbidity (less than 100 NTU) accompanied by a decline in the flow rate. The subsequent increase in turbidity at an increased hydraulic gradient of 16.6 was less than 100 NTU. However, as shown in Fig. 5, the effluent turbidity rapidly increased again at a hydraulic gradient of 33.3, which was also accompanied by the highest increase in flow rate. It is assumed, therefore, that this hydraulic gradient has exceeded the critical value,  $i_{cr}$  for base soil erosion. Moreover, the inspection of dried out effluent at each pressure increment also confirmed that the maximum base soil erosion occurred under this value of  $i_{cr}$ . With further increase in hydraulic gradients up to

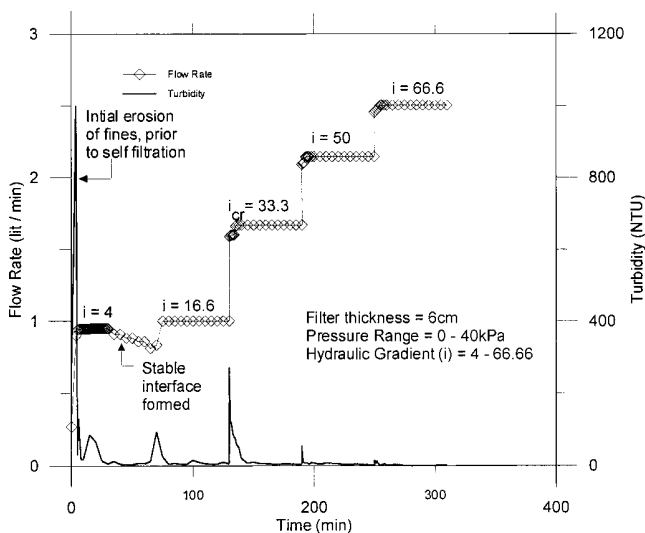


**Fig. 5.** Flow rate and turbidity with time for the filter type  $C_u = 1.45$  and compaction time 15 s

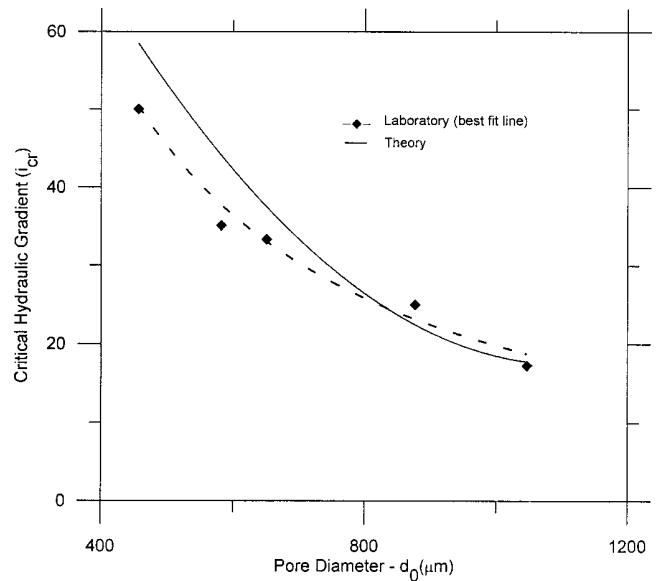


**Fig. 6.** No erosion boundaries based on critical hydraulic gradients for  $d < d_0$ , for a constant  $d$  value of (250  $\mu\text{m}$ )

66.7, the subsequent turbidity peaks were much smaller, because, most of the base soil has already been eroded under the  $i_{cr}$  of 33.3.

For a filter thickness of 6 cm subjected to vertical flow, the experimental values of  $i_{cr}$  for increasing pore diameter are plotted in Fig. 6 together with the predictions based on Eq. (14). For the saturated base soil, submerged unit weight ( $\gamma'$ ) was determined to be 8.2 kN/m<sup>3</sup>. The experimental results are in good agreement with the theory. This verifies that the critical hydraulic gradient ( $i_{cr}$ ) for a given base soil-filter combination can be determined using Eq. (14) for cohesionless materials.

## Conclusion

In this paper, a mathematical formulation was introduced to calculate the critical hydraulic gradient ( $i_{cr}$ ) required for base particle movement within a filter. Each base particle smaller than the filter pore diameter will start to move under this critical hydraulic gradient governed by its own submerged unit weight, grain size and particulate friction. The value of  $i_{cr}$  determined here is different from that proposed in a previous study by Indraratna and Vafai (1997), where drag force acting on the base particle was excluded in the hydrodynamic force component. The validity of analytical theory predicting the critical hydraulic gradient was examined on the basis of the behavior of uniform fine gravel filters, retaining a fine base sand. For vertical flow, the experimental results verified the authors' model. However, for cohesive base soils, the magnitude of  $i_{cr}$  required for particle movement is expected to be greater, and the authors are in the process of extending the current model for cohesive base soils.

## References

- Kovacs, G. (1981). *Seepage hydraulics*, Elsevier Scientific, Amsterdam.
- Indraratna, B., and Vafai, F. (1997). "Analytical model for particle migration within base soil-filter system." *J. Geotech. Geoenviron. Eng.*, 123(2), 100–109.